

First results from a dense semi-continuous GPS deployment during the September 2005 northern Cascadia slow slip event

Sarah K. Thompson

Richard A. Bennett

Sigrún Hreinsdóttir

Department of Geosciences, University of Arizona, Tucson, Arizona, USA

Daniel J. Johnson*

*Deceased. Formerly Department of Earth and Space Sciences, University of Washington, Seattle, Washington, USA

In August of 2005, we deployed 29 GPS stations in the Olympic Peninsula with the goal of recording crustal motion associated with a slow slip event on the Cascadia subduction interface. This is the first semi-continuous GPS network established with the aim of providing a high resolution image of crustal motion associated with a slow slip event. We recorded data during the period from August 2 to October 20, roughly centered on the slow slip event that began between September 3-6 and lasted for approximately 14 days. We observe transient surface motions associated with this event at 27 stations bounded by the surface projection of the 20-70 km slab contours. The total observed surface displacements range from about 2 to 9 mm. The precise time of onset of transient motion is difficult to discern from the observed coordinate time series, but our results are consistent with the onset of crustal motion coinciding with the time of first tremor detection. Maximum surface displacements are centered on the Strait of Juan de Fuca, including southern Vancouver Island and the northern Olympic Peninsula, the region directly overlying the arch in the Juan de Fuca plate. Coastal sites located above the 20 km and shallower slab contour record little or no deformation during the 2005 event, providing a new constraint on the down-dip limit of the locked part of the subduction interface. We present simple elastic dislocation models to illustrate the dependence of the observed motions on the time of rupture initiation, propagation rate and direction.

1. Introduction

Continuous GPS (CGPS) networks, especially those located along convergent margins, have recently shown that the notion of elastic rebound envisioned by *Reid* [1911] provides a limited understanding of fault mechanics; some fraction of the elastic strain that accumulates around faults during the interseismic period is now known to be quasi-periodically released during transient aseismic slip events occurring on the deeper parts of the major plate boundary faults (e.g., *Dragert* [2001] and many subsequent papers). These slow slip events, known as Episodic Tremor and Slip (ETS) result in observable deformation transients accom-

panied by seismic tremors can be used to investigate the frictional properties of the fault zone [*Liu and Rice*, 2005; *Lowry*, 2006]. Significant observational and theoretical work indicates that slow slip events will occur in the transition zones between stable and unstable sliding [*Scholz*, 1998], and may thus be a feature of many or even all fault zones, although there is no assurance that such events must be of sufficient frequency of occurrence or of sufficient amplitude to be observable for all fault zones.

An underlying question surrounding the interpretation of ETS is how exactly the tremor and the slip relate to one another. One interpretation of this relationship is that the tremor and the retrograde slip are different manifestations of a single process [*Shelly*, 2007]; alternatively, another interpretation is that two observations are separate yet simultaneous phenomena if fluid flow is the source process for the tremor. In Cascadia, observations of S-wave polarization in the direction of plate convergence supports the theory that the tremor is caused by slip on the plate interface [*Wech and Creager*, 2007]. Furthermore, slow slip is linked to upper plate structure based on the correlation between geologic terrane and segmentation/reoccurrence interval of ETS [*Brudzinski*, 2007] and the correlation between forearc basins and areas where ETS occurs [*Fuller*, 2006].

One of the fundamental limitations in our present understanding of the relationship between tremor and slip phenomena has been the sparse nature of existing CGPS and seismic networks. To address this limitation, we conducted a semi-continuous GPS survey within the Olympic Peninsula region with the goal of capturing a predicted slow slip event on the Cascadia subduction interface. The GPS experiment coincided with a dense seismic deployment [*Wech and Creager*, 2007]. The goal of this paper is a first analysis of the GPS data collected during the 2005 experiment and a comparison with results from the seismic experiment.

2. GPS Deployment and Data Analysis

We conducted our experiment using 29 GPS units from UNAVCO's TopCon GB-1000 campaign pool. Topcon PG-A1 antennas were mounted on galvanized stainless steel rods driven into the ground from 1-2 m, sufficient for the short-term stability required for the experiment. Antennas were located from 30 to 100 cm above the ground surface. The systems were powered by a combination of solar panels and two 18 amp-hr gel cell batteries and were left to collect data autonomously for approximately 100 days. GPS stations were spaced ~20 km apart on average, and the total aperture of the network was ~150 km. All equipment including the monuments were removed at the end of the experiment.

We processed the data using the GAMIT/GLOBK software package (version 10.3) along with all available regional CGPS stations, including data from the Pacific Northwest Geodetic Network (PANGA)/Plate Boundary Observatory (PBO) Nucleus, Western Canada Deformation Array (WCDA), and PBO networks. The length of the data files decreased as the experiment continued due to diminishing solar power supply associated with shorter days and increased cloud coverage, resulting in higher scatter towards the end of the experiment and after the event. These data were processed along with a set of over 200 globally distributed reference stations in order to better constrain the solution. In total, we analyzed data from 47 stations whose velocities are defined within the Stable North American Reference Frame (SNARF).

3. Results

Due to the short length of the semi-continuous time series (< 4 months), the total displacement is calculated by differencing average daily position estimates for the seven days preceding and seven days following the September 2005 ETS event. From the coordinate time series we determine that the 2005 event initiated after Sep. 6 \pm 2 days and concluded by Sep. 21. Sites located from southernmost Vancouver Island, in regions between the surface projection of the 25 - 65 km slab contour intervals, up to 47.5°N record crustal motion associated with the transient slip event. Coastal sites located in the region near the surface projection of the 20 km slab depth contour (P401, OL21) did not record the slow slip event, delineating the down-dip limit of the seismogenic zone.

Total offsets range from nearly undetectable (less than 1 mm) to a maximum of 9 mm at station OL18 (a station with high scatter). Stations with the largest displacements are clustered around the northernmost portions of the Olympic Peninsula and southern Vancouver Island. These stations typically had total displacement values of 5-6 mm. The displacement vectors are dominantly in the southwest direction, opposite of the interseismic deformation field. The three most southerly sites in the semi-continuous network (OL13, OL07, and OL03) record a counter-clockwise rotation of the transient displacement field, with the displacement vectors point southeast. These stations are located near the southern segment of the Hurricane Ridge fault, marking the southern boundary of the 2005 ETS region and further linking ETS to upper plate structure, as suggested by *Brudzinski* [2007].

We forward model dislocations on the thrust interface along a transect cross-cutting the axis arch of the subducting Juan de Fuca slab, directly beneath the Olympic Mountains. This approach allows us to further investigate the relationship between seismic tremor and geodetic slip by comparing model results from various rupture scenarios to our GPS coordinate time series. Synthetic time series are created from successive static surface displacement computations using the methodology of *Okada* [1985]. Each dip-slip perturbation represents a new data point in the time series, where each iteration corresponding to an arbitrary time step which is scaled to represent various rupture velocities. The synthetic time series represent the modeled surface displacement at an observation point directly above the 30 km slab contour, corresponding to GPS sites which recorded a distinct transient slip signal.

For the up-dip and down-dip models, the subduction interface is parameterized into nine fault tiles based upon the geometry of *McCrorry* [2004] with lengths (in strike direction) of 200 km to minimize edge effects. The width (in dip direction) of each fault segment is \sim 5.9 km, with depths

ranging from \sim 35-47 km. The dip ranges from \sim 12.7-15.5°, depending upon the distance along the transect. In the along-strike model the dislocation passes beneath the observation point with a rupture propagation path parallel to the model strike direction. In this model, the subduction interface is parameterized into ten 20 km long (in strike-direction) fault patches spanning the slab depth range of 31-49 km, dipping \sim 13°. The total span of the along-strike rupture path is 180 km, with 90 km offset on either side of the transect.

4. Discussion

A total slip value of 3.15 cm minimizes misfit between the model and the E-W displacement for site OL28 (Sol Duc Springs). Site OL28 was selected due to its characteristic time series for sites located above the 30 km slab depth. This value is less than the inverted maximum slip of 3.8 cm for the 2003 slow slip event determined by *Melbourne* [2005] although of the same order of magnitude. An inversion for slip distribution for this event would likely yield a greater value than 3.15 cm; in this case, however, to test for time series sensitivity to rupture directivity and velocity, this simplistic case is sufficient.

The initial tremor burst occurred on September 3 up-dip from the 50 km slab contour at the arch of the subducting plate and migrated up-dip to just below the 30 km slab contour, over a period of about 10 days [*Wech and Creager*, 2007]. The total distance travelled up-dip was approximately 100 km. Once the tremor reached its up-dip limit, it propagated bi-directionally; the northern segment propagated northwest below the southern tip of Vancouver Island until September 30; the southern segment propagated until September 15 [*Wech and Creager*, 2007].

While the exact onset time is difficult to ascertain from GPS time series, we determined that the event initiated around September 6 \pm 2 days and lasted until September 21, although the scatter was high near the end of September across the entire network. This independent determination of event duration correlates well with the tremor observations, especially considering that the southerly-propagating segment passes below the most concentrated portion of our network and is therefore most representative of the slip source for displacements observed within the Olympic Peninsula.

The synthetic time series for the up-dip and along-strike rupture models each have a distinct appearance. The along-strike synthetic time series appears the most realistic based on the character of the time series, with a critical point in the middle where the rate of change changes from positive to negative, as shown in Figure 3. Sum squared residuals (SSR) were calculated for each model using data from OL28 over the time period of 9/06 to 9/21. The 20 km/day along-strike rupture model had a SSR of 7.15, while the up-dip rupture model (\sim 6km/day) had a slightly higher SSR value of \sim 8.4. Tremor locations were used to constrain the rupture direction because of the similarity of the SSR statistic. In contrast different rupture velocities for the up-dip model yielded larger differences in the SSR. Therefore, we chose to further test for the rupture velocity in the along-strike model since the geometry of our network is such that our sites are most sensitive to the along-strike slip propagation. Velocities of 40, 20, 13, 10, 7 were analyzed; among them, the 20 km/day model had the lowest SSR, which slightly greater than the tremor propagation velocity of \sim 15 km/day roughly estimated from the results of *Wech and Creager* [2007].

5. Conclusion

The displacement field shown here represents the densest record to date of a transient slip event in all of Cascadia. This experiment marks the first time that a campaign-style deployment successfully captured a predicted slow slip

event. In the past, geodetic experiments required years of observation in order to attain results. This experiment is unique in that after only a short semi-continuous style deployment, a phenomenon was successfully recorded with greater resolution than ever before.

Areas with the greatest amount of slip coincide with the surface projection of the arch in the Juan de Fuca plate. These data further delineate the southern extent of the slipping region in addition to the down-dip extent of the seismogenic zone. The peculiar counter-clockwise rotation of displacement vectors at the southernmost stations recording the transient deformation further link ETS to upper plate structure.

Synthetic time series were produced by computing the value at one observation point along the profile corresponding to 30 km above the slab interface. The cumulative displacement value at the observation point for model iteration is plotted as a function of some arbitrary time constant. This time constant was scaled to represent various rupture velocities. We computed the SSR statistic for five different along-strike rupture velocities, ranging from 7–40 km/day. The 20 km/day rupture model minimized the SSR.

The approach presented here is a first attempt to determine rupture direction and velocity from GPS coordinate time series on a station by station basis. Dense GPS networks will continue to address this in greater detail. These results are consistent with the notion that slow slip and tremor are coincident with each other.

Acknowledgments. During the course of this experiment, Dr. Daniel Johnson passed away. His warm personality is greatly missed by all who knew him. The authors thank the many individuals who assisted with the deployment and retrieval of this network. We acknowledge the UNAVCO Facility, the UNAVCO PBO Facility, and the Olympic National Park for their assistance. This project was funded by the NSF EarthScope Program grant number EAR-0545519.

References

- Brudzinski, M. R., Allen, R. M. (2007), Segmentation in episodic tremor and slip all along Cascadia, *Geology*, 35(10), 907–910, 10.1130/G23740A.1.
- Dragert, H., Wang, K., and T. S. James (2001), A silent slip event on the deeper Cascadia subduction interface, *Science*, 292.
- Dragert, H., Wang, K., and Rogers, G. (2004), Geodetic and seismic signatures of episodic tremor and slip in northern Cascadia subduction zone, *Earth Planets Space*, 56, 1143–1150.
- Fuller, C. W., Willett, S. D., Brandon, M. T. (2006), Formation of forearc basins and their influence on subduction zone earthquakes, *Geology*, 34, 65–68, 10.1130/G21828.1.
- Kao, H., Shan, S., Dragert, H., Rogers, G. Cassidy, J. F., and Ramachandran, K. (2005), A wide depth distribution of seismic tremors along the northern Cascadia margin, *Nature*, 436, 841–844.
- Liu, Y., Rice, J. R. (2005), Aseismic slip transients emerge spontaneously in three-dimensional rate and state modeling of subduction earthquake sequences, *J. of Geophys. Res.*, 110, B08307, 10.1029/2004JB003424.
- Lowry, A. R. (2006), Resonant slow fault slip in subduction zones forced by climatic load stress, *Nature*, 442, 802–805.
- McCausland, W., Malone, S., Johnson, D. (2005), Temporal and spatial occurrence of deep non-volcanic tremor: From Washington to northern California, *Geophys. Res. Letters*, 32, L24311, 10.1029/2005GL024349.
- McCrorry, P. A., Blair, J. L., Oppenheimer, D. H., Walter, S. R. (2004), Depth to the Juan de Fuca slab beneath the Cascadia subduction margin: A 3-D model for sorting earthquakes, *U.S. Geological Survey Data Series*, 91.
- Melbourne, T. I., Szeliga, W. M., Miller, M. M., Santillan, V. M. (2005), Extent and duration of the 2003 Cascadia slow earthquake, *Geophys. Res. Letters*, 32, L04301, 10.1029/2004GL021790.
- Okada, Y. (1985), Surface deformation due to shear and tensile faults in a half-space, *Bull. Seismo. Soc. of Am.*, 75, 1135–1154.
- Reid, H. F. (1911), The Elastic-Rebound Theory of Earthquakes. *University of California Publications, Bulletin of the Department of Geology*, 6, 19.
- Scholz, C. H. (1998), Earthquakes and friction laws, *Nature*, 391, 37–42.
- Shelly, D. R., Beroza, G. C., Ide, S. (2007), Non-volcanic tremor and low-frequency earthquake swarms, *Nature*, 446, 305–307.
- Wech, A. G., and Creager, K. C. (2007), Cascadia tremor polarization evidence for plate interface slip, *Geophys. Res. Letters*, 34, L22306, 10.1029/2007GL031167.

S. K. Thompson, Department of Geosciences, University of Arizona, Gould-Simpson Building 77, Tucson, AZ 85721, USA. (skt@email.arizona.edu)

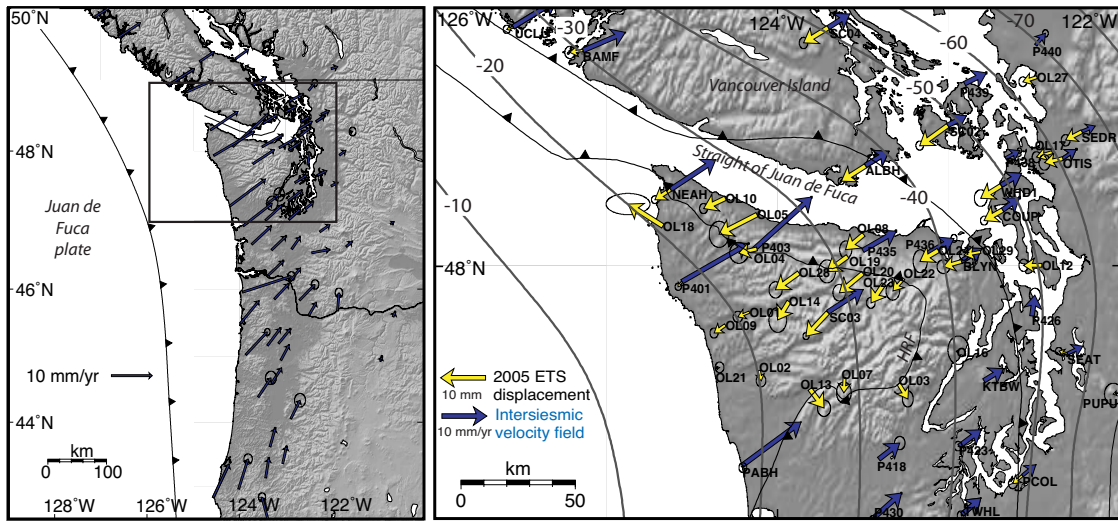


Figure 1. *Left panel:* Regional velocity field; Velocities relative to the Stable North American Reference Frame. *Right panel:* Inset showing the Olympic Peninsula. Displacement field for the September 2005 slow slip event (yellow arrows) superimposed on the interseismic velocity field (blue arrows) from CGPS stations. Hurricane Ridge Fault (HRF) plotted to show counterclockwise rotation of transient displacement vectors at the southern portion of the fault zone. Slab Contours after McCrory [2004].

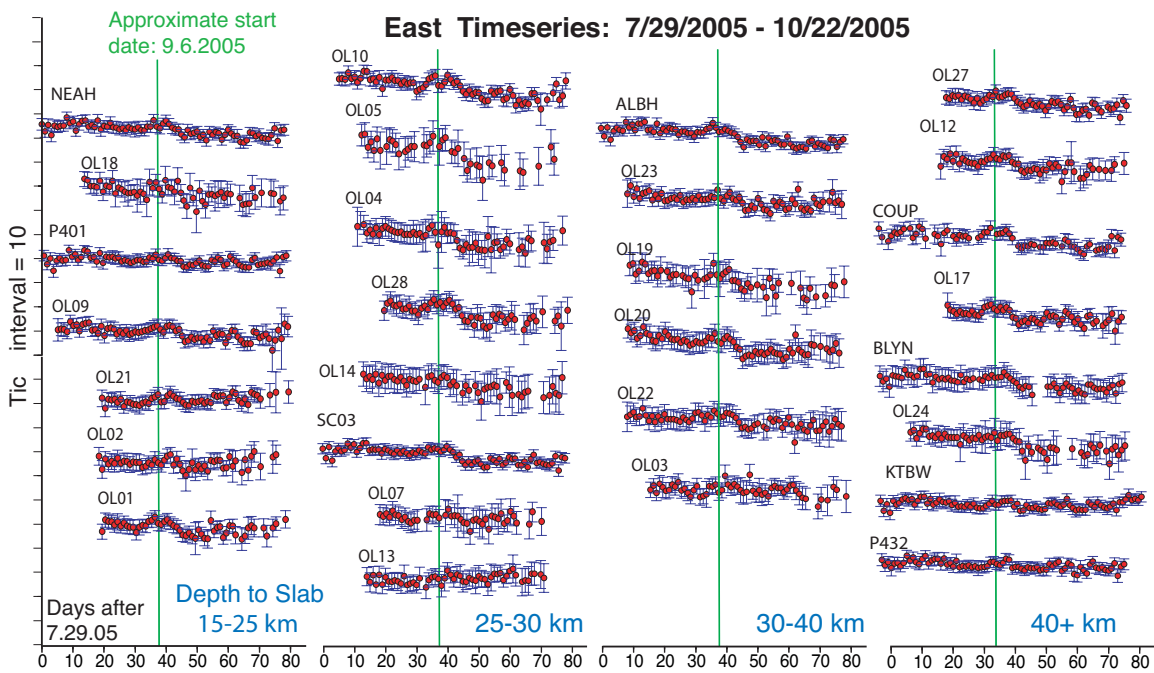


Figure 2. Selected time series, arranged according to depth above slab.

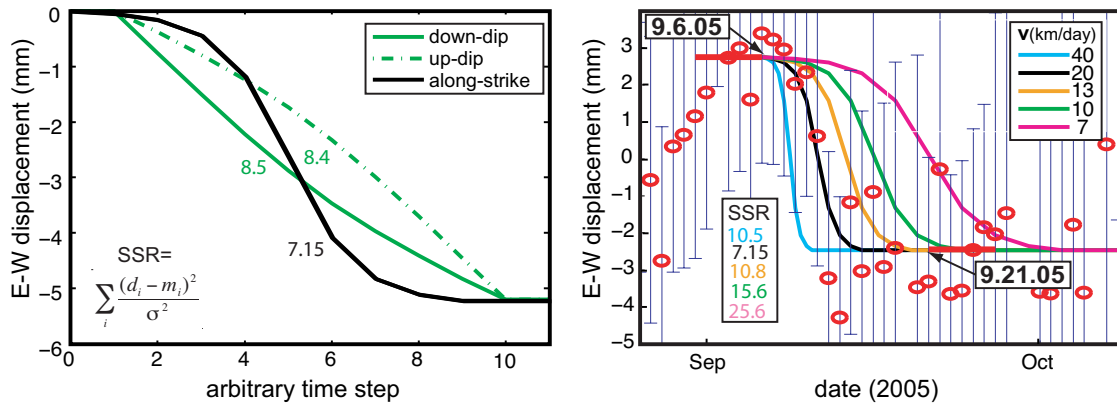


Figure 3. Synthetic time series computed from Okada’s analytical solution [1985] for surface displacement above the 30 km slab contour due to a 3.15 cm dislocation on the subduction thrust between the 50 and 30 km slab contour intervals. Geometry of subduction interface after McCrory [2004]. *Left panel:* up-dip vs. down-dip and along-strike propagation, with Sum Squared Residual (SSR) values calculated between model and data from OL28. *Right panel:* data from OL28 and synthetic time series for different rupture velocities of the along-strike rupture model.